



Physics Section, University of Geneva

Studies of readout electronics and optical elements for a gamma-ray telescope

Nicolas De Angelis

Supervisors: Prof. Teresa Montaruli, Dr. Matthieu Heller

July 12, 2019



Outline

- ① Introduction: Gamma-ray astrophysics with Imaging Atmospheric Cherenkov Technique and the CTA SST-1M telescope
- ② Optimisation of the pulse shape for the LVR3 sensor via front-end electronics simulation
- ③ Characterisation of the MUSIC readout ASIC with the LVR3 and LCT5 sensors
- ④ Characterisation of the uniformity of the entrance window of the camera
- ⑤ Conclusions and Outlooks

Section 1

Introduction: Gamma-ray astrophysics with
Imaging Atmospheric Cherenkov Technique
and the CTA SST-1M telescope



Credit: ESO



Multi Messenger Astronomy

Cosmic
Rays



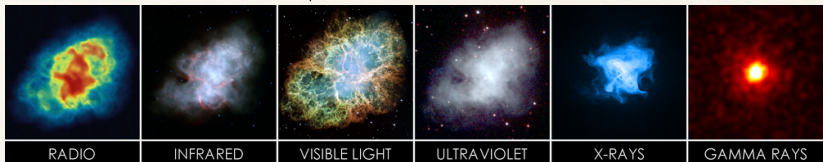
Photons



Neutrinos



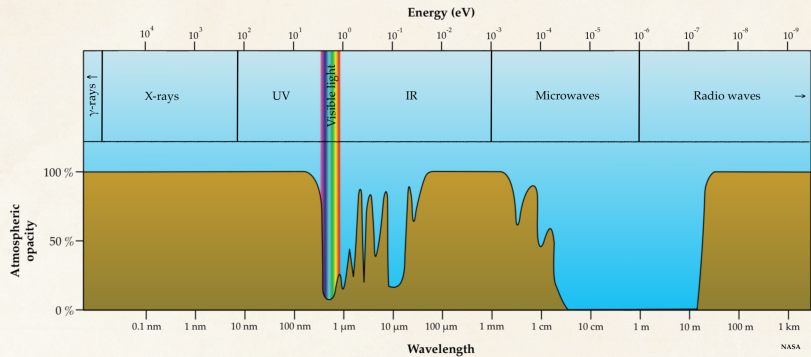
Gravitational
waves



Sources: Radio: NRAO/AUI and M. Bietenholz, J.M. Uson, T.J. Cornwell; Infrared: NASA/JPL-Caltech/R. Gehrz (University of Minnesota); Visible: NASA, ESA, J. Hester and A. Loll (Arizona State University); Ultraviolet: NASA/Swift/E. Hoversten, PSU; X-ray: NASA/CXC/SAO/F. Seward et al.; Gamma: NASA/DOE/Fermi LAT/R. Buehler



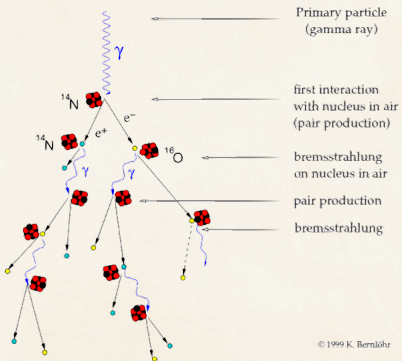
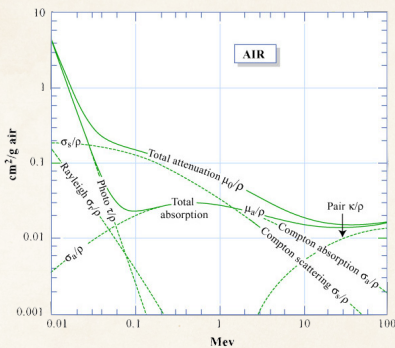
Detection of Gamma-Rays





Detection of Gamma-Rays

Interaction of Gamma-Rays Photons with Atmosphere

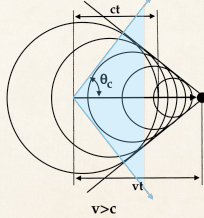
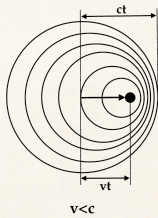
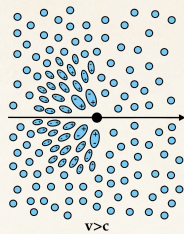
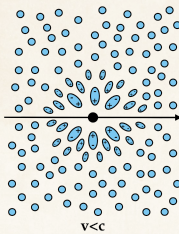


© 1999 K. Bernlöhr



Imaging Atmospheric Cherenkov Technique

The Cherenkov effect



- If $v > c$, a light cone is emitted with aperture:

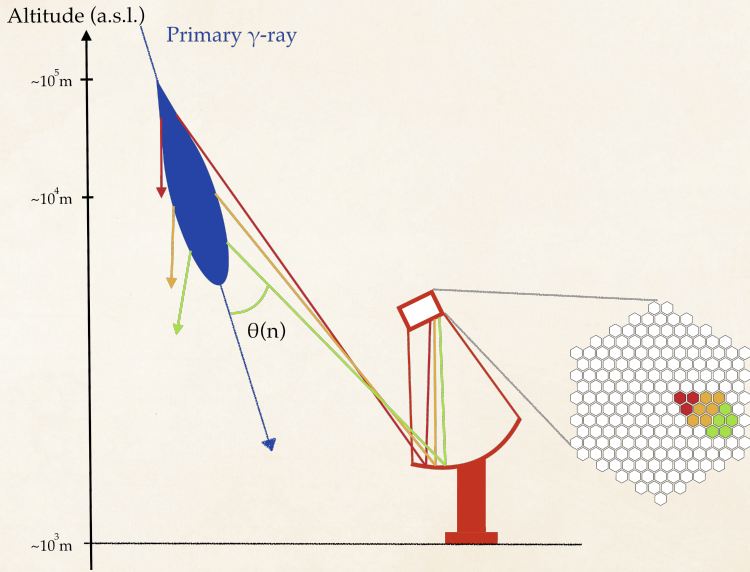
$$\cos \theta_C = \frac{1}{\beta n}$$

- Intensity of the light (Franck-Tamm formula):

$$\frac{dN}{dx} = 2\pi\alpha Z^2 \int \left(1 - \frac{1}{\beta^2 n^2}\right) \frac{d\lambda}{\lambda^2}$$



Imaging Atmospheric Cherenkov Technique





Imaging Atmospheric Cherenkov Technique

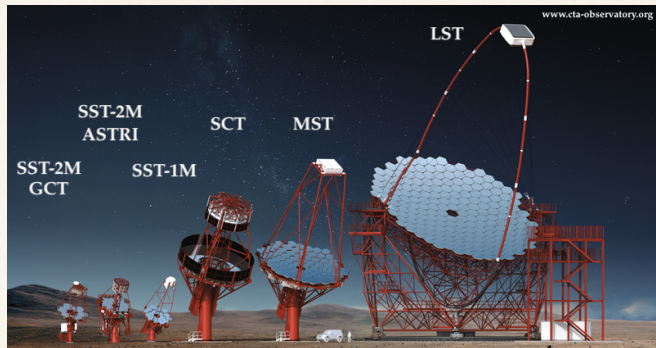
Current experiments



	HESS	VERITAS	MAGIC
Location	Namibia	Arizona, USA	La Palma, Spain
Hemisphere	South	North	North
Number of telescopes	5	4	2
Field of View	5°	3.5°	3.5°
Energy range	30 GeV - 100 TeV	50 GeV - 50 TeV	30 GeV - 100 TeV
Telescope diameter	4 × 12 m + 1 × 18 m	4 × 12 m	2 × 17 m



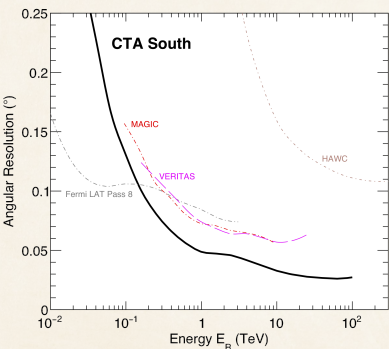
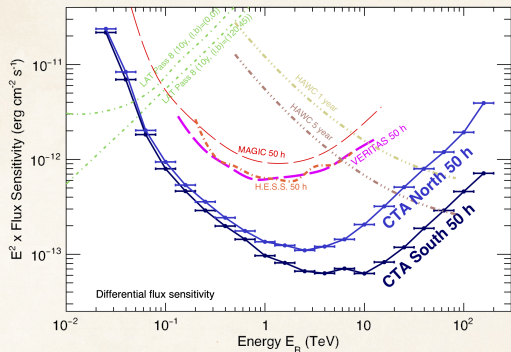
The Cherenkov Telescope Array (CTA)



	LST	MST	SST
Energy range	20 GeV - 150 GeV	150 GeV - 5 TeV	5 TeV - 300 TeV
Number of telescopes	4 South + 4 North	25 South + 15 North	70 South
Primary reflector diameter	23.0 m	11.5 m	4.0-4.3 m
Field of View	4.3°	7.5°	8.3 – 10.5°
Sensors	PMT	PMT	SiPM



The Cherenkov Telescope Array (CTA) Performances

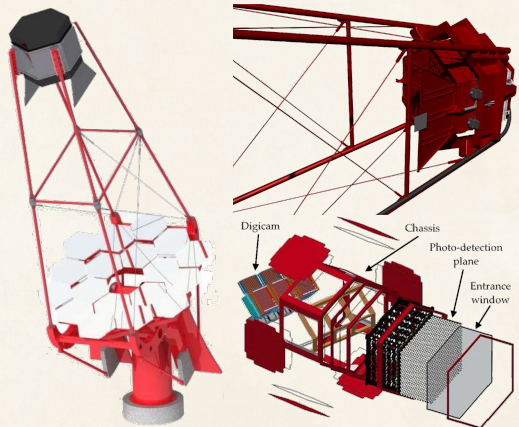


cta-observatory.org



CTA SST-1M telescope and camera

- 8.6 tons telescope, 200 kg camera
- 4 m diameter, 5.6 m focal length
- Angular pixel size 0.24°
- Davies-Cotton design
- Mirrors: 18 hexagonal facets

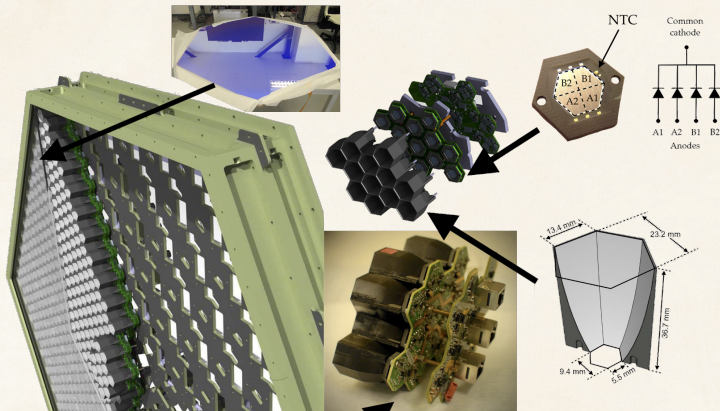


Heller, Matthieu, et al. "An innovative silicon photomultiplier digitizing camera for gamma-ray astronomy."

The European Physical Journal C 77.1 (2017): 47.



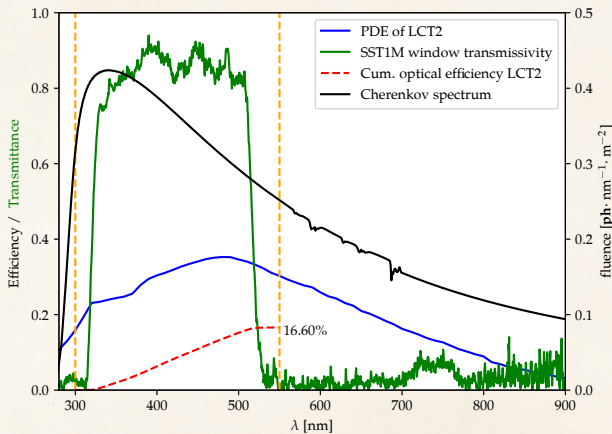
CTA SST-1M telescope and camera PhotoDetection Plane (PDP)



Heller, Matthieu, et al. "An innovative silicon photomultiplier digitizing camera for gamma-ray astronomy." The European Physical Journal C 77.1 (2017): 47.



Camera Optical Efficiency Requirement



- Optical efficiency requirement updated (B-TEL-1170 Photon Detection Efficiency) → must be >20%

Section 2

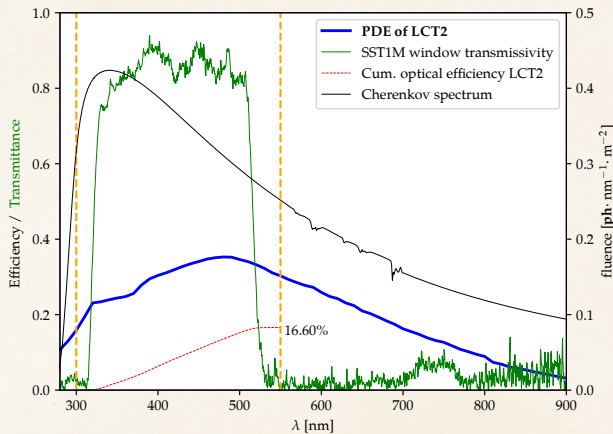
Optimisation of the pulse shape for the
LVR3 sensor via front-end electronics
simulation



Credit: ESO



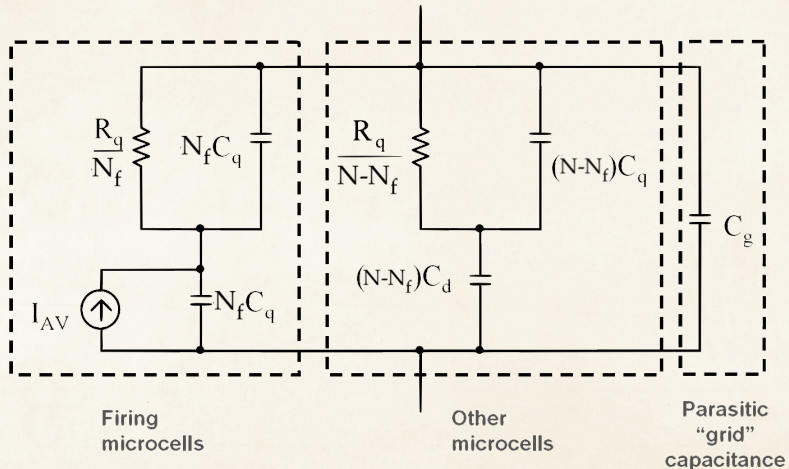
Camera Optical Efficiency Requirement



- Optical efficiency requirement updated (B-TEL-1170 Photon Detection Efficiency) → must be >20%



SiPM pulse shape model: the Corsi model

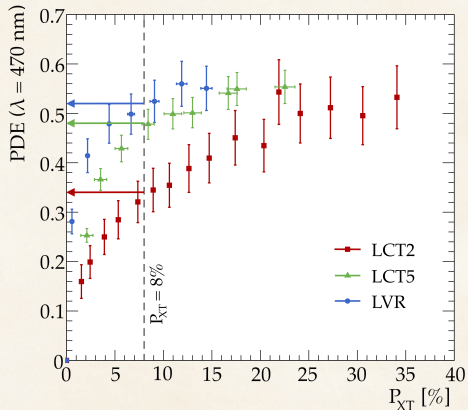


Corsi, F., et al. "Electrical characterization of silicon photo-multiplier detectors for optimal front-end design." 2006 IEEE Nuclear Science Symposium Conference Record. Vol. 2. IEEE, 2006.



Candidates for SST-1M sensor upgrade

- SST-1M camera currently working with LCT2 sensor operated at 8% cross talk probability \implies PDE=34%
- Photo-detection efficiency can be improved by changing the sensor:
 - LCT5: PDE($P_{XT}=8\%$)=48%
 - LVR3: PDE($P_{XT}=8\%$)=52%

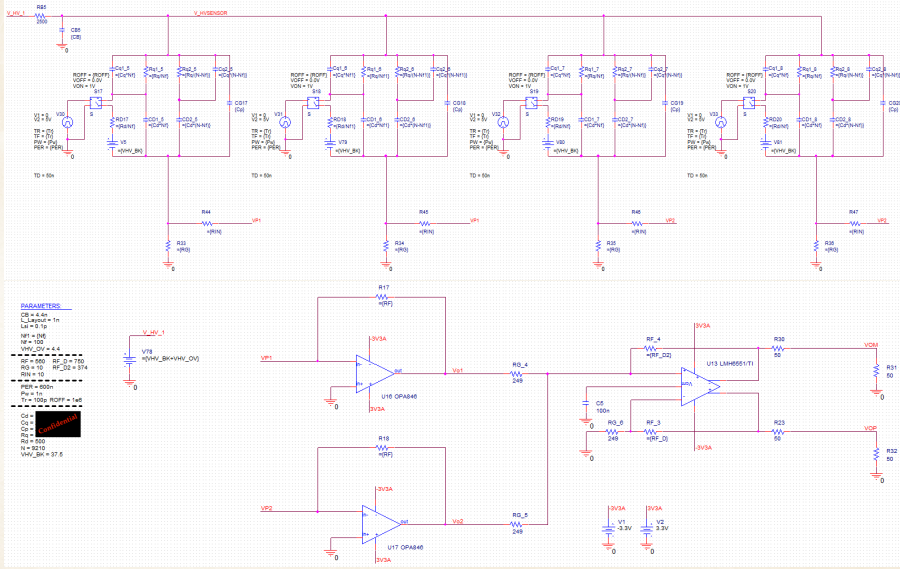


Measurements from A. Nagai

- LCT = Low Cross Talk, LVR = Low Voltage Resistor
- S10943, called LCT2 for 2nd generation sensor based on LCT technology from Hamamatsu
- S13360, called LCT5 for 5th generation sensor based on LCT technology from Hamamatsu
- S14520, called LVR3 for 3rd generation sensor based on LVR technology from Hamamatsu



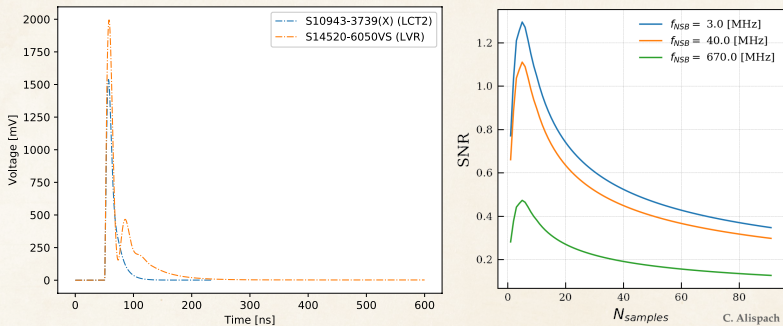
PSpice model of the electronics





LCT2 vs. LVR3 pulse shapes

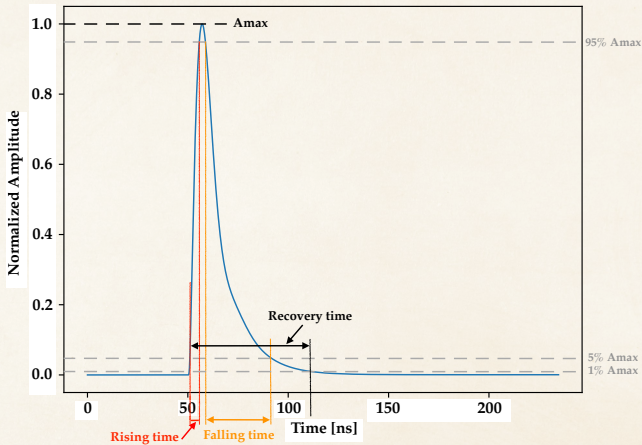
Parameter	T _{rec} [ns]	t _{fall} [ns]	t _{rise} [ns]	Charge	A _{max} [mV]
LCT2 pulse	52.3	32.3	4.69	$2.35 \cdot 10^{-8}$	1538
LVR3 pulse	148.6	75.6	5.41	$4.40 \cdot 10^{-8}$	1995



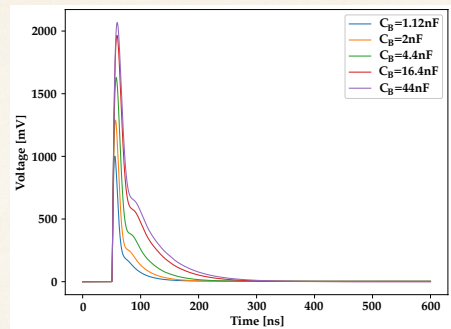
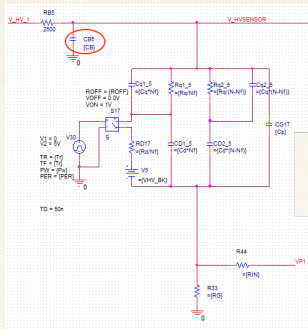
CTA requirement on integration window (B-SST-1210): "signal integration must be possible within a time window of between 20 and 30 ns with respect to the Camera trigger time for signals in the range 0-400 photons"



Characterisation of the pulse shape



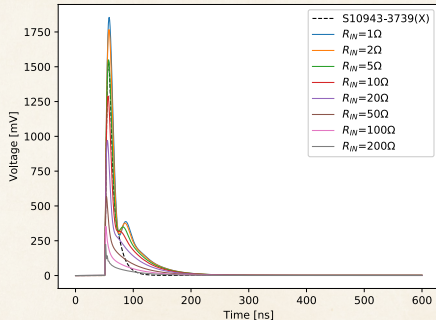
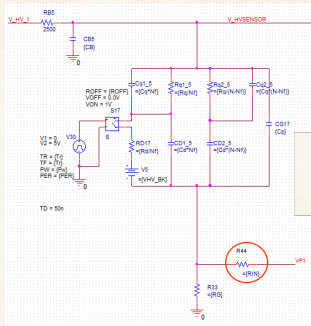
Pulse shape evolution with C_B



- Decreasing $C_B \implies$ decreasing SNR

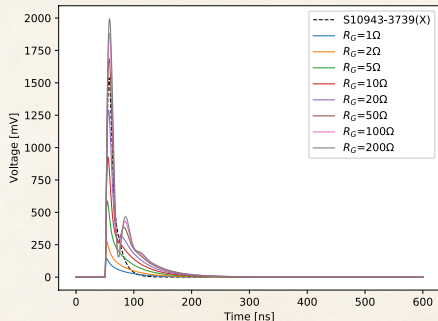
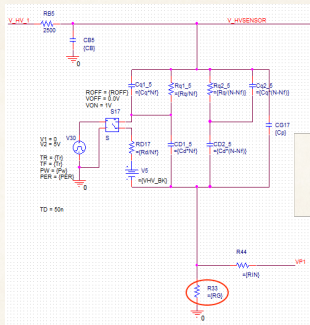


Pulse shape evolution with R_{IN}



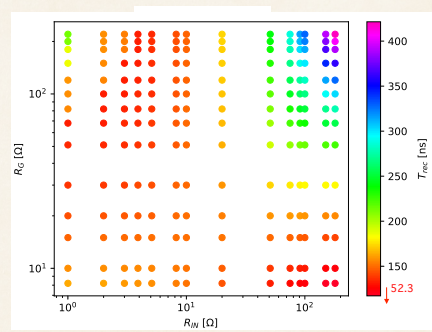
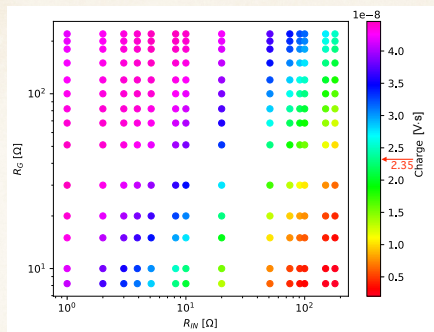


Pulse shape evolution with R_G



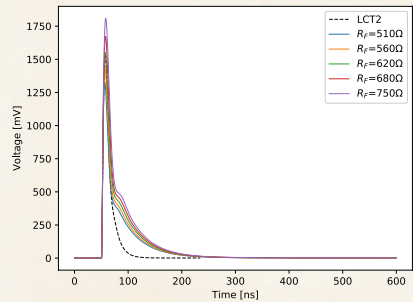
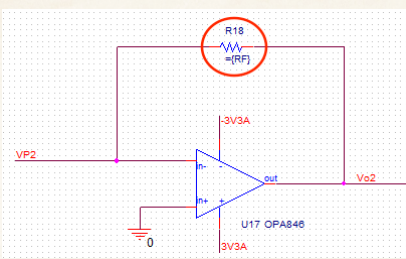


Charge and recovery time vs. (R_{IN} , R_G)

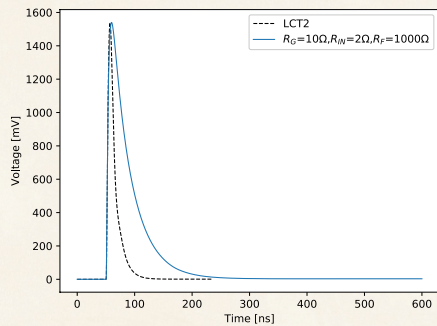
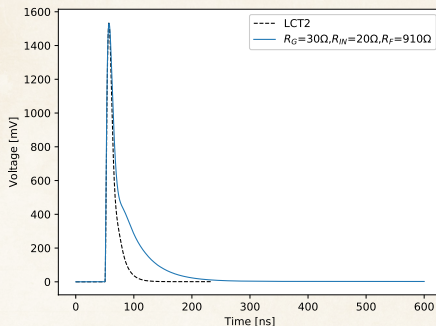




Pulse shape evolution with R_F



Shortest achieved well-behaved pulses

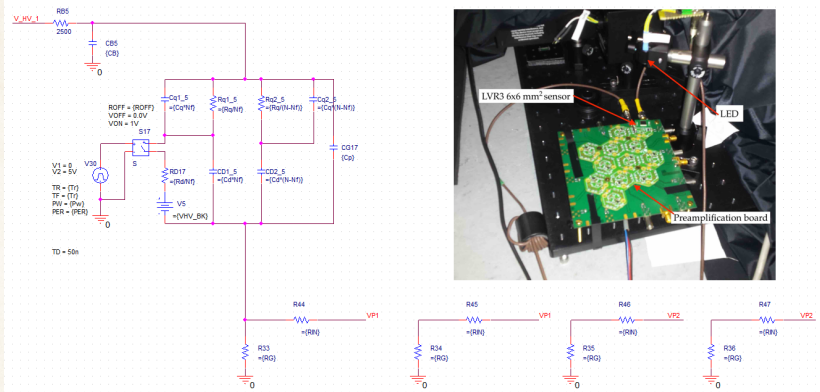


R_{IN} [Ω]	R_G [Ω]	R_F [Ω]	T_{rec} [ns]	t_{rise} [ns]	t_{fall} [ns]	A_{max} [mV]	Charge [V·s]
2	10	1000	176.9	5.906	102.2	1540	$6.82 \cdot 10^{-8}$
20	30	910	167.0	4.683	92.00	1532	$4.49 \cdot 10^{-8}$
10	200	560	52.3	4.69	32.3	1538	$2.35 \cdot 10^{-8}$



Faithfulness of the model

Measurement and simulation of a 6x6 sensor

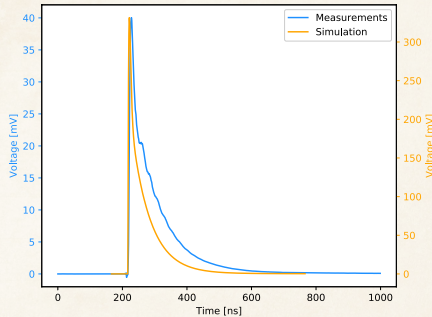




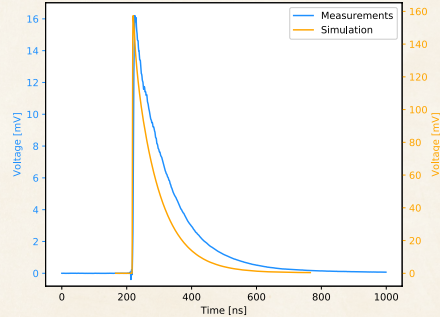
Faithfulness of the model

Comparison of measured and simulated pulses

$(R_{IN} = 20 \Omega, R_G = 100 \Omega)$



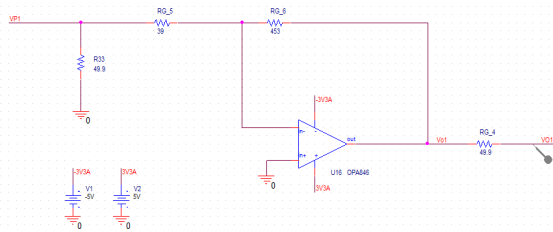
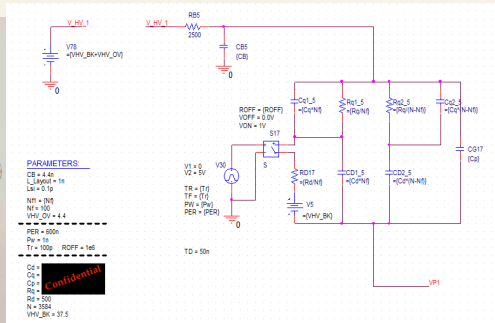
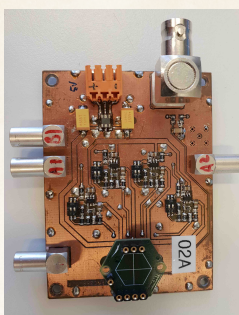
$(R_{IN} = 51 \Omega, R_G = 100 \Omega)$





Faithfulness of the model

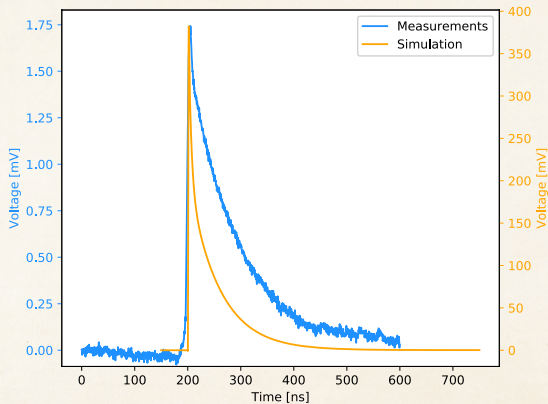
Simulation of a single channel PCB





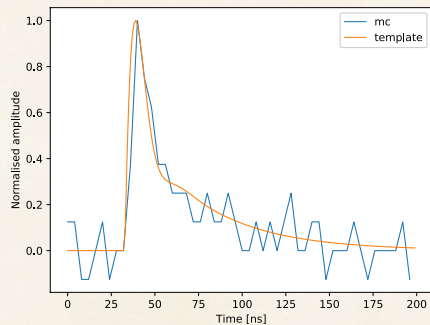
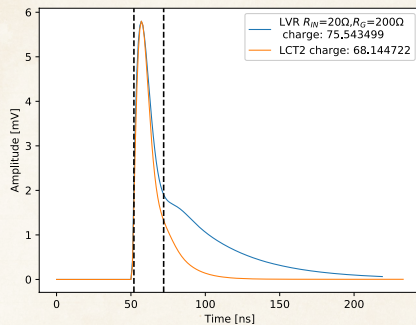
Faithfulness of the model

Pulse shape with the single channel PCB



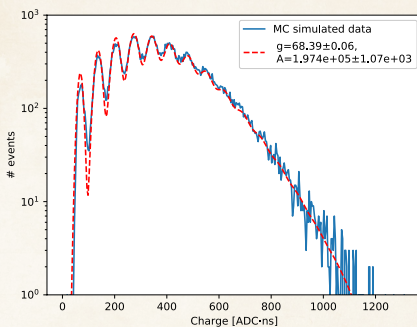


Monte Carlo Simulation of DigiCam

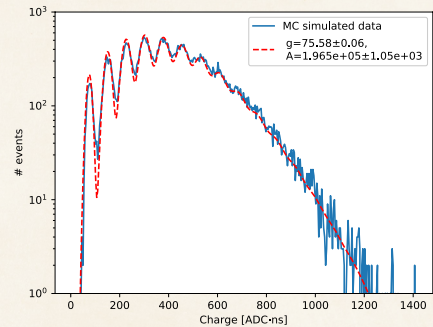


Photon counting ability

LCT2



LVR3



$$\text{MPE fit: } f(x) = A \sum_{n=0}^N P(n|\mu, \lambda) \left[\frac{1}{\sqrt{2\pi}\sigma_n} e^{-\left(\frac{x-n\cdot g}{\sqrt{2}\sigma_n}\right)^2} \right]$$

with $P(n|\mu, \lambda) = \frac{\mu(\mu+\lambda n)^{n-1} \exp(-\mu-n\lambda)}{n!}$ and $\sigma_n = \sqrt{\sigma_e^2 + n\sigma_1^2}$.

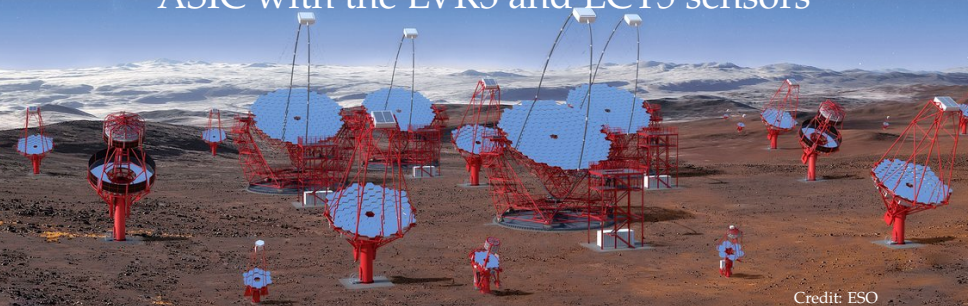


Conclusions on the PSpice study

- LVR3 induces very long pulses due to its large capacitance and to its larger quenching resistance (microcell capacitance of 128 fF vs. 85 fF for LCT2, R_q is 2.3 times bigger for LVR3 than for LCT2)
- Optimisation of the preamplification stage not enough to reduce recovery time down to the required 20-30 ns
- Pulses even longer with measurement → either bad OPA simulation or Corsi model not fair enough
- Despite longer pulse, photon counting ability seems to be similar for LVR3 than for LCT2 → but should be worse for measured pulses

Section 3

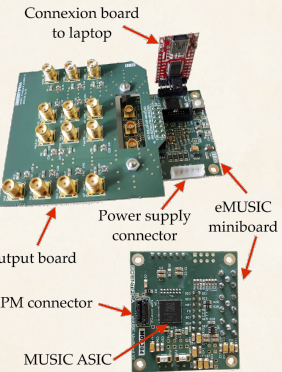
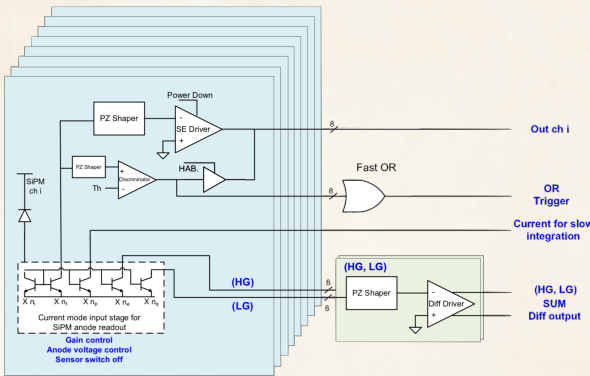
Characterisation of the MUSIC readout
ASIC with the LVR3 and LCT5 sensors



Credit: ESO



The MUSIC readout ASIC

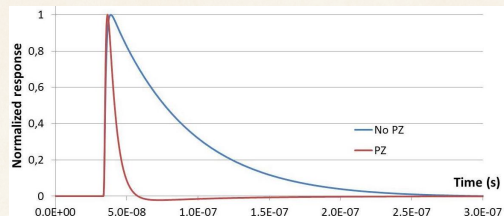
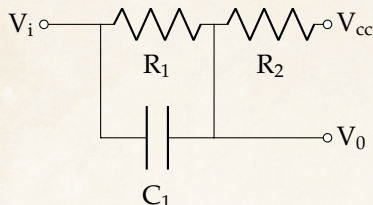


Gómez, Sergio, et al. "MUSIC: An 8 channel readout ASIC for SiPM arrays." Optical Sensing and Detection IV. Vol. 9899. International Society for Optics and Photonics, 2016.



The MUSIC readout ASIC

Pole Zero Cancellation

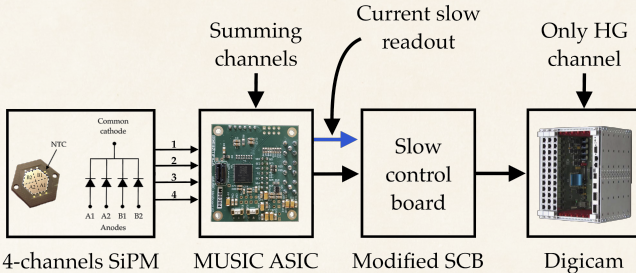


- Resistance ladder
R1/R2 take values listed in the table
- 5bit capacitance ladder (C1) follows a linear distribution starting at 1.2pF with steps of 0.1pF

R _{lad}	R ₁ (low atten OFF) [kΩ]	R ₁ (low atten ON) [kΩ]	R ₂ [Ω]
0	46.50	18.60	7650
1	48.30	20.40	5850
2	50.10	22.20	4050
3	51.90	24.00	2250
4	52.35	24.45	1800
5	52.80	24.90	1350
6	53.25	25.35	900
7	53.70	25.80	450



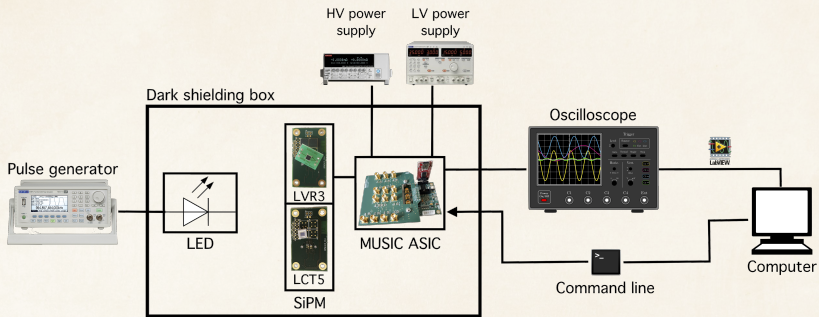
Integration of MUSIC in the camera



- 1 output channel per pixel \Rightarrow 1 MUSIC to sum the 4 anodes of a single pixel \Rightarrow 1 MUSIC per pixel \Rightarrow save power (100 mW per pixel instead of 400 mW), a bit more expensive (increase of 2% of the telescope cost)
- Currently DC coupled \rightarrow MUSIC is AC coupled \Rightarrow we have to use the slow readout current to monitor baseline shifts
- SCB needs to be modified to readout slow integration output



MUSIC measurement setup



```
>> mini_music.exe config -P COM13 -e 0 -u 0 -t -a -p R C
```

Changing configuration of the ASIC

Serial port used to communicate with MUSIC board

Channels to be enabled (single ended outputs)

Channels to be summed (differential outputs)

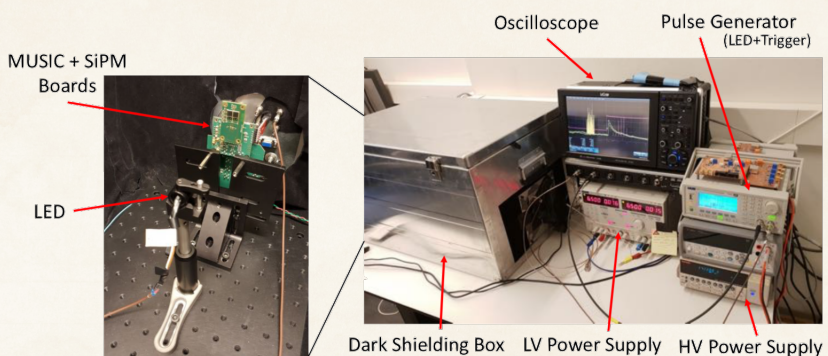
High transimpedance mode (HG)

Enable PZ filters (R from 0 to 7 & C from 0 to 31)

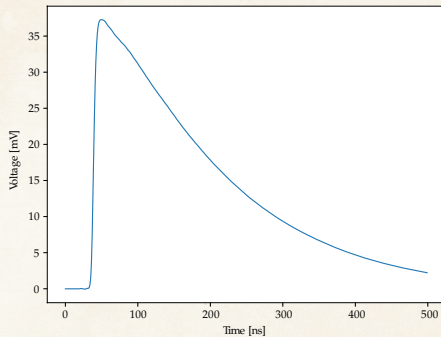
Reduce PZ attenuation



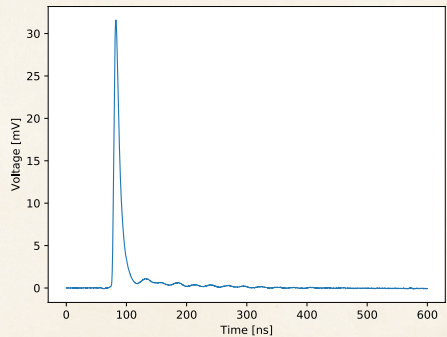
MUSIC measurement setup



No PZ cancellation



PZ cancellation R=4, C=9

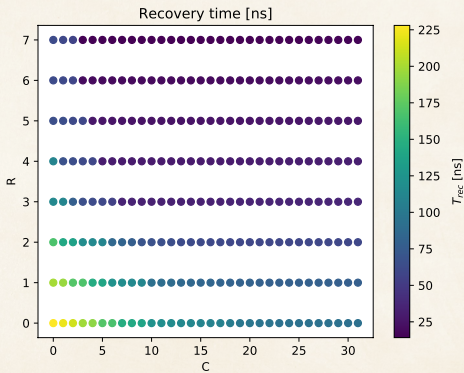




PZ cancellation with LVR3 sensor

Recovery time

- Integration window
20-30 ns (CTA
requirement)
- Without PZC, LVR3 6x6
pulse recovery time (1 to 1
%) is 400 ns

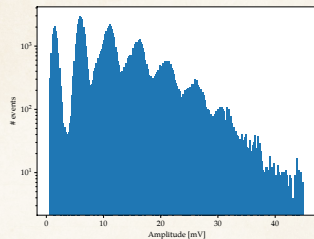




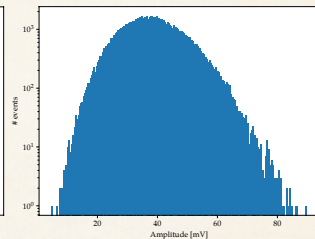
PZ cancellation with LVR3 sensor

Sensitivity to single photon

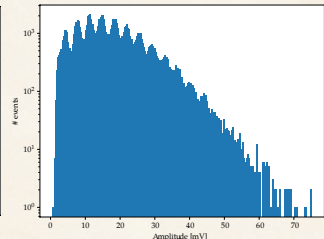
LVR3 3x3 mm²
 $(\Delta V = 4.4V)$



LVR3 6x6 mm²
 $(\Delta V = 4.4V)$



LVR3 6x6 mm²
 $(\Delta V = 7V)$

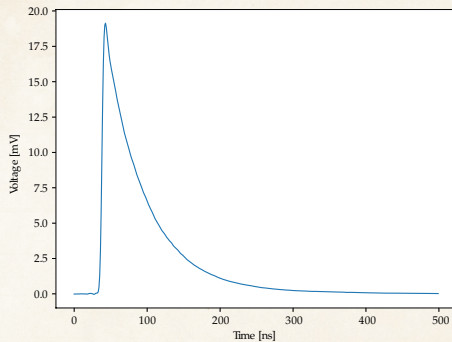


Having a reasonable photon sensitivity would require to work with an over-voltage of at least 7 V and then increase the cross talk probability from 8% to 15%

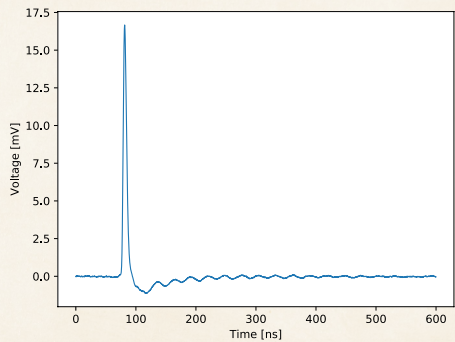
PZ cancellation with LCT5 sensor

Pulse shape before vs. after PZ

No PZ cancellation



PZ cancellation R=4, C=9

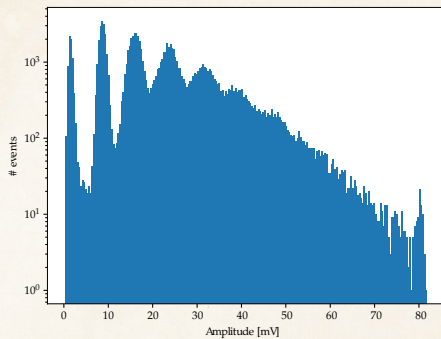




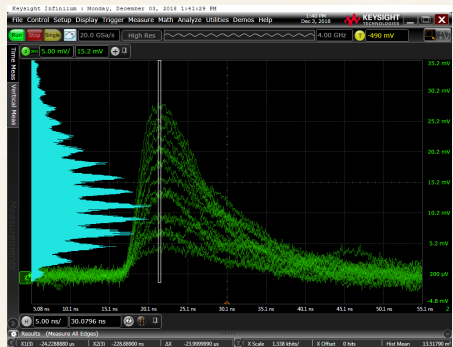
PZ cancellation with LCT5 sensor

Sensitivity to single photon

LCT5 3x3 mm²



LCT5 6x6 mm²

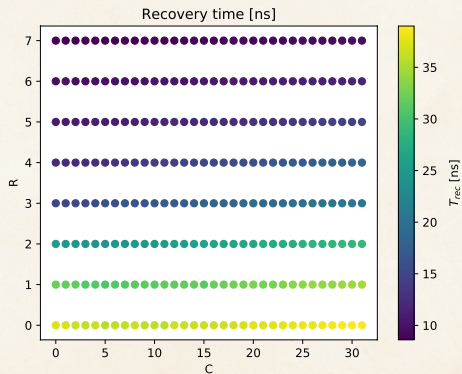




PZ cancellation with LCT5 sensor

Recovery time

- Integration window
20-30 ns (CTA
requirement)
- Without PZC, LCT5 3x3
pulse recovery time (1 to 1
%) is 120 ns



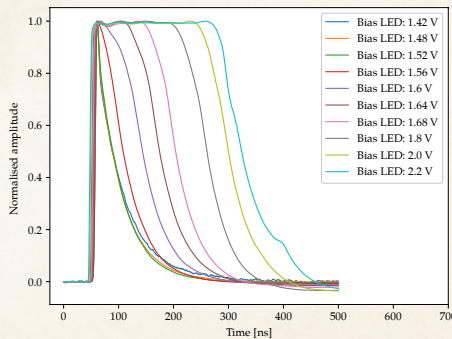


Saturation behavior with LCT5

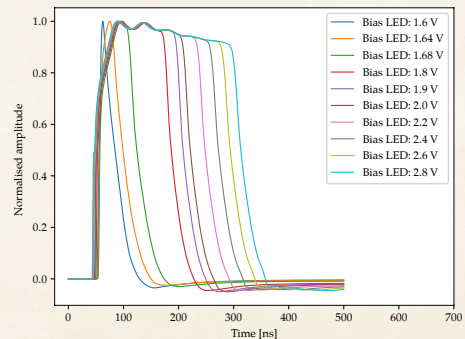
Pulse shapes for increasing light level

Using differential outputs:

High Gain



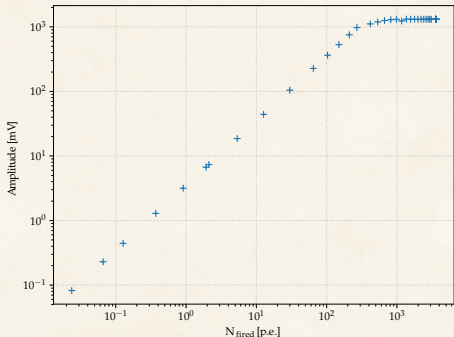
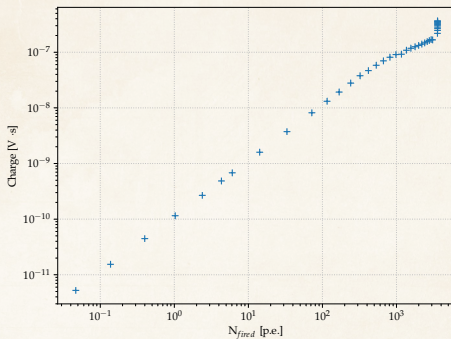
Low Gain





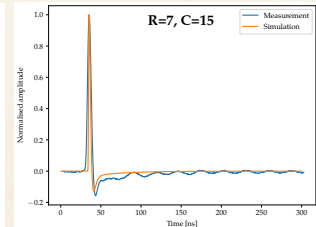
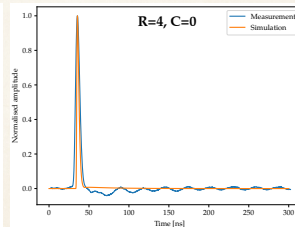
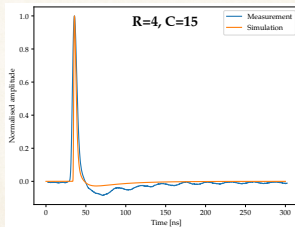
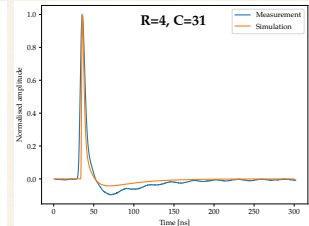
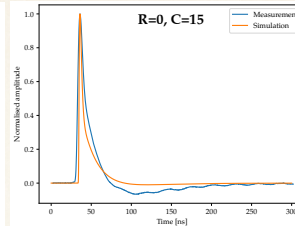
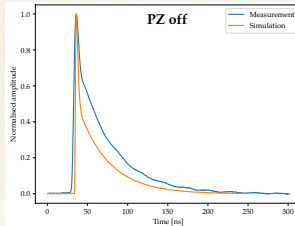
Saturation behavior with LCT5

Calibrated linearity plots



- Good linear behavior below saturation for both amplitude and charge
- Charge still linear above saturation until 2000 photons
- Allow to reconstruct signal even above saturation with good accuracy

Simulation of the MUSIC ASIC LCT5 pulse shapes



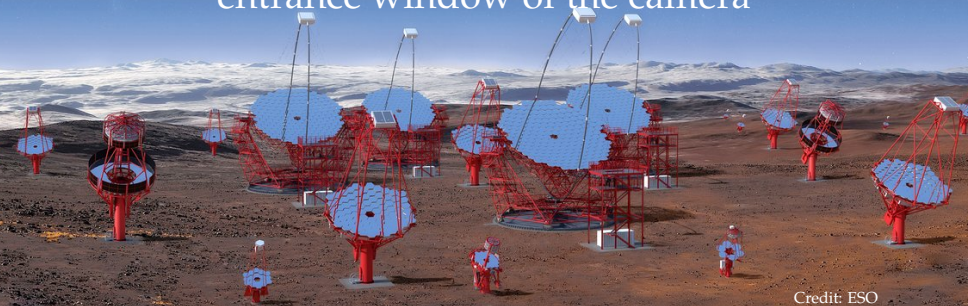


Conclusions on MUSIC

- LVR3 not suitable for our application → even if PZC allow short pulses, not able to see single photons
- LCT5+MUSIC could be a good solution for SST-1M
 - PDE from 34% to 48% by replacing LCT2 by LCT5
 - Applying PZC allow very short pulses (less than 30ns)
 - Able to see single photons
 - Good behavior in saturation
 - Very good agreement for the pulse shape between measurements and simulations
- Using MUSIC would allow to reduce power consumption (100 mW/pix instead of 400 mW/pix is using one ASIC per pixel)
- Using MUSIC would require to redesign the SCB for baseline shift monitoring
- MUSIC more expensive than current preamplification electronics (increase of 2% on the overall telescope cost)

Section 4

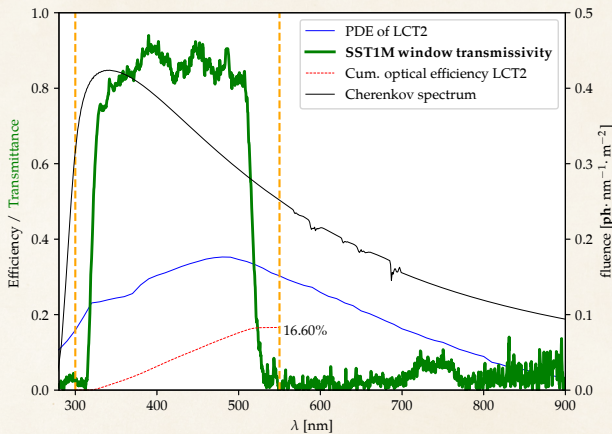
Characterisation of the uniformity of the entrance window of the camera



Credit: ESO



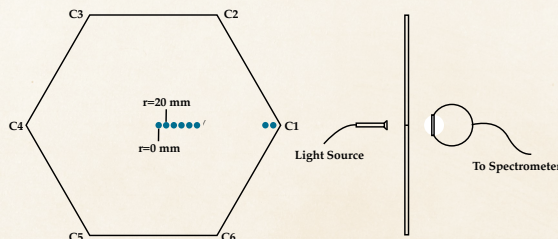
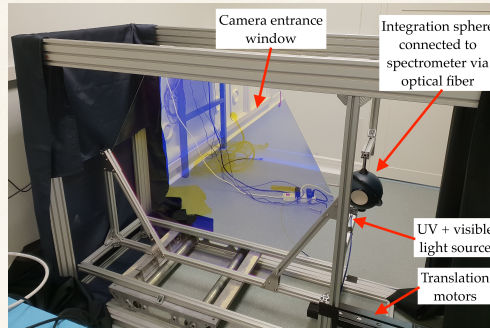
Camera Optical Efficiency Requirement



- Optical efficiency requirement updated (B-TEL-1170 Photon Detection Efficiency) → must be >20%

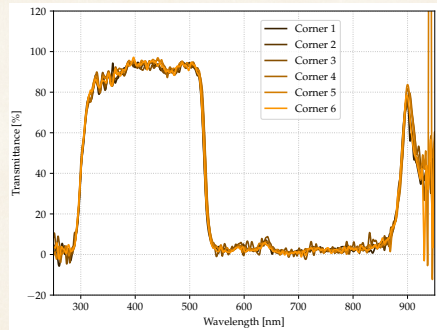
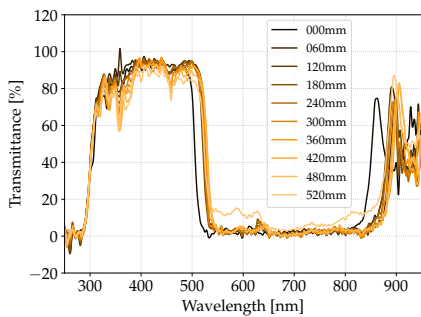


Measurement setup



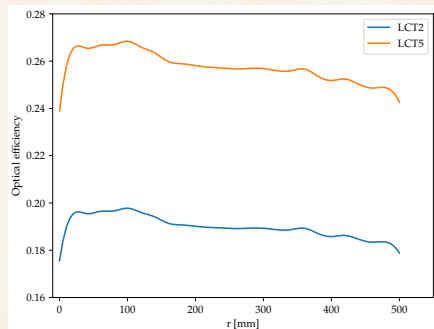
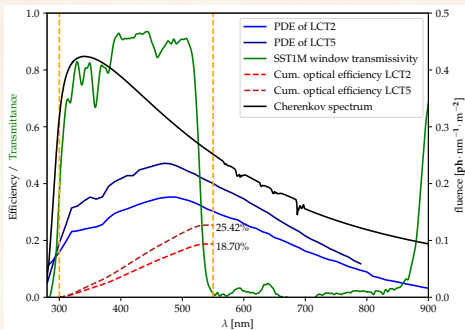


Evolution of the spectrum across the window



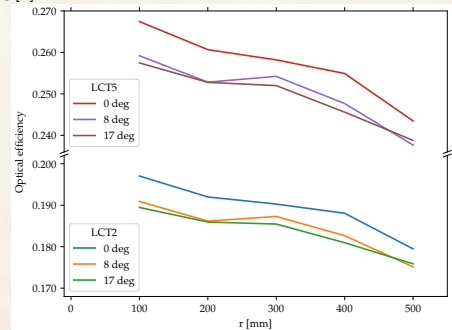
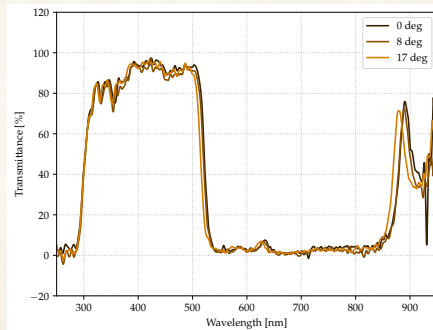
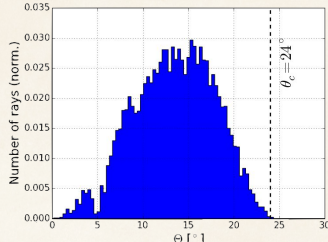


Optical efficiency of the new window



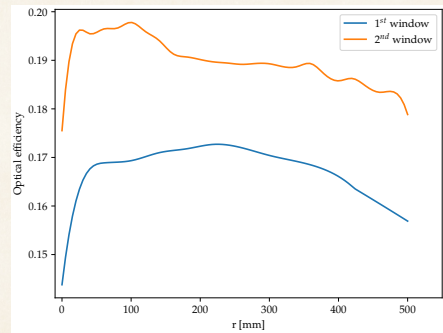
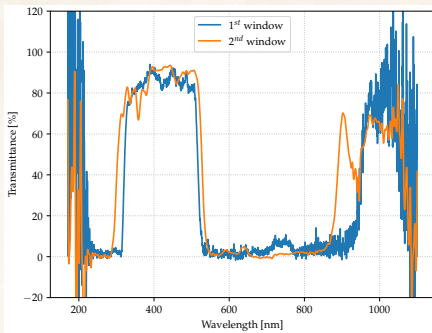


Angular dependency



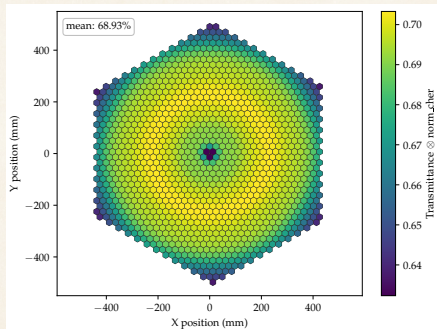
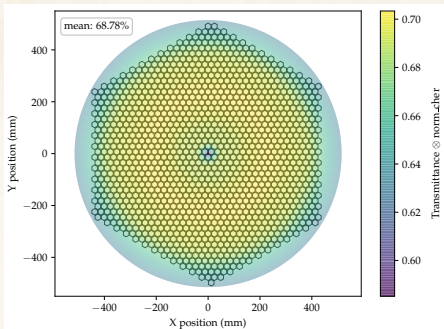


Comparison with the first window





Extraction of the mean transmittance for each pixel (for the 1st window)

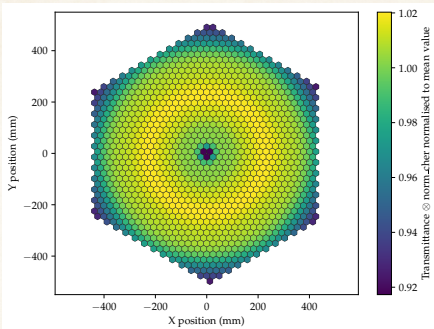




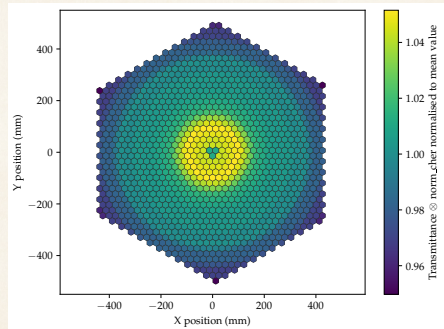
Impact of non-uniformity on image reconstruction

Extraction of the flat-fielding factors

1st window



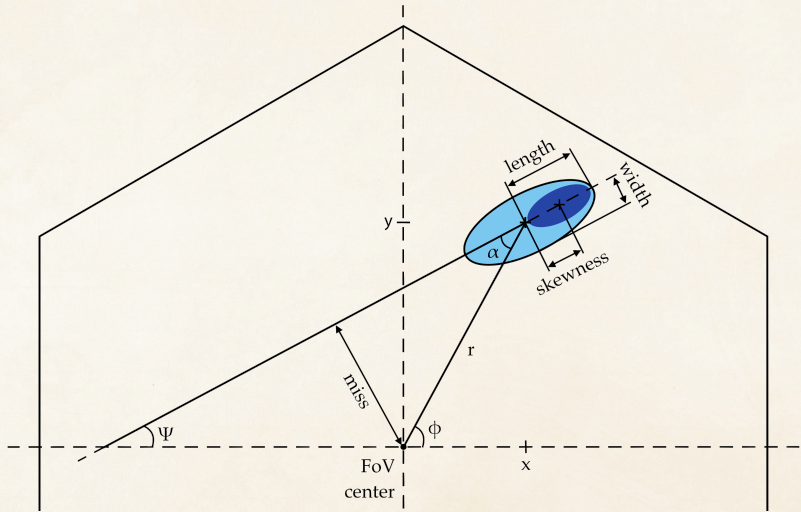
2nd window





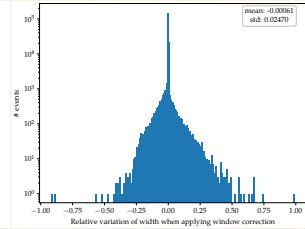
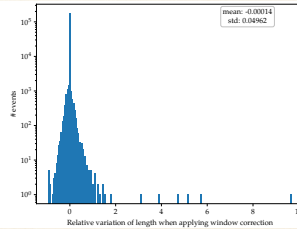
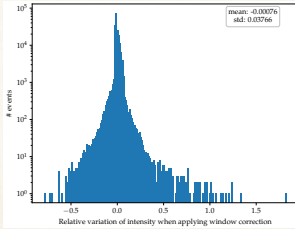
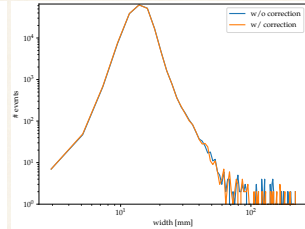
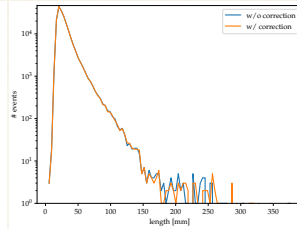
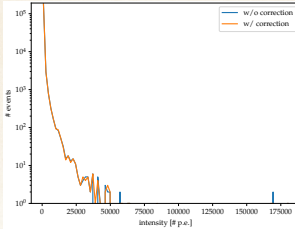
Impact of non-uniformity on image reconstruction

Image parametrisation



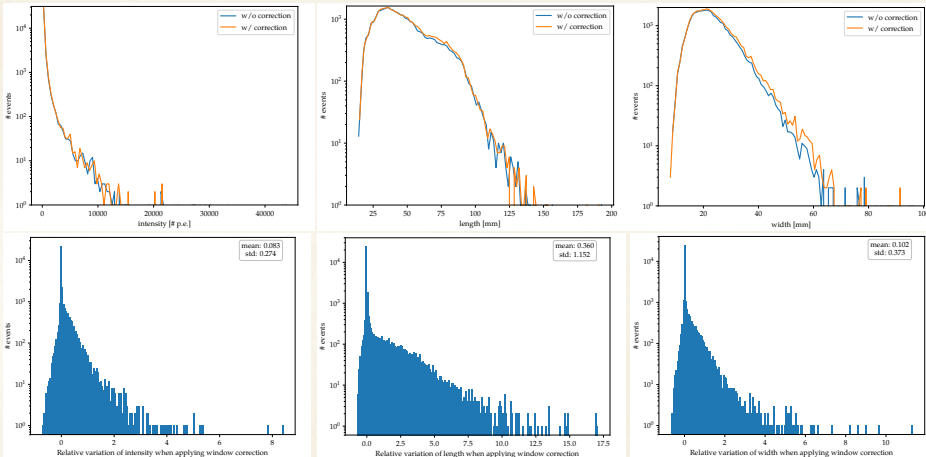


Impact of non-uniformity on real data





Impact of non-uniformity on simulated showers



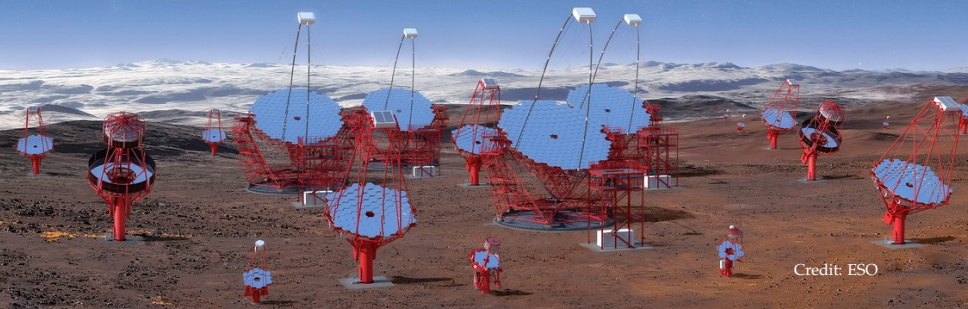


Conclusions on the entrance window

- Transmittance spectrum has been improved with the new window → improvement of the lower bound \Rightarrow better optical efficiency
- Uniformity across the window also better
- Improvement of spectrum not enough to pass the 20% required optical efficiency → sensor upgrade still needed
- Non-uniformity has a small impact on observation data but a bigger impact on simulated on-axis showers
- Non-uniformity of entrance window now accounted in the camera pipeline

Section 5

Conclusions and Outlooks



Credit: ESO



Conclusions and Outlooks

- LVR3 not suitable for our application (too long recovery time)
- LCT5+MUSIC is a nice candidate for sensor/electronics upgrade
- MUSIC would also allow to save power (100 mW instead of 400 mW per pixel)
- SCB redesign needed to monitor baseline shift since MUSIC is AC coupled
- Redesign of MUSIC to allow sub-summations in order to have one ASIC for \sim 3-4 pixels
- Entrance window uniformity and transmittance have been improved
- Non-uniformity of window is now accounted in the analysis chain



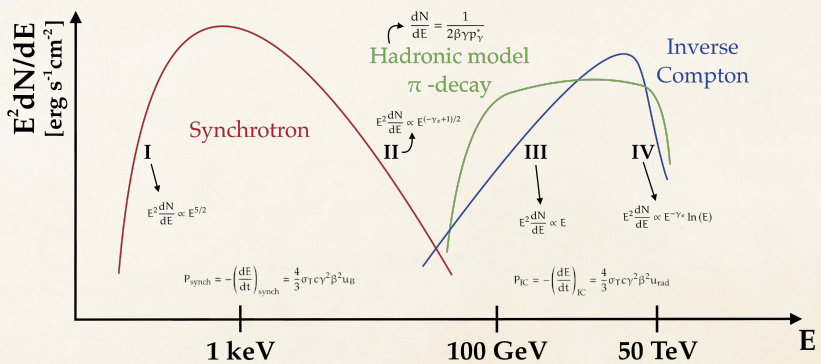
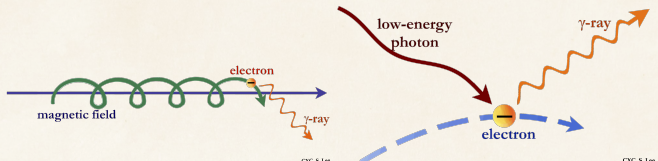
A wide-angle photograph of a radio telescope array, likely the Square Kilometer Array (SKA), situated in a dry, arid landscape. The array consists of numerous large dish antennas, each mounted on a red support structure. Some dishes are blue, while others are red. The background features a dark, star-filled sky with a prominent central band of the Milky Way.

Questions ?



Backup slides

Gamma-Ray Production Processes

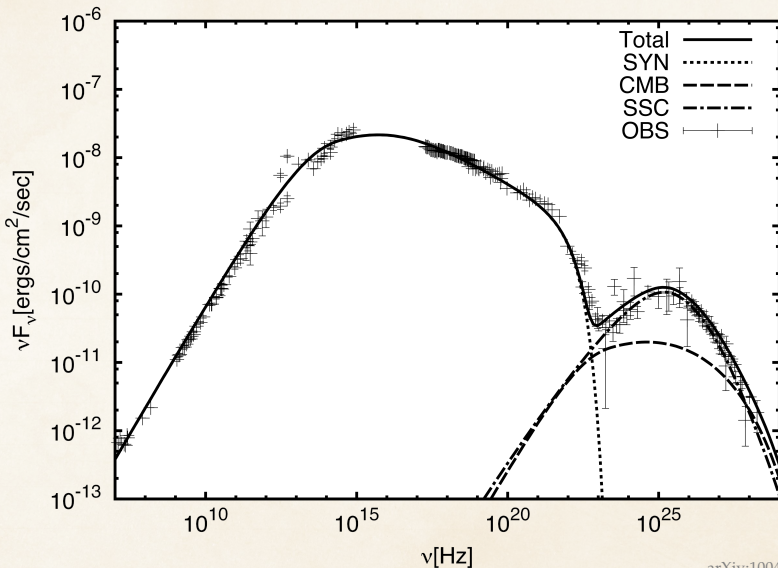


Spurio, Maurizio. Particles and Astrophysics: A Multi-messenger Approach. Springer, 2016.



Backup slides

Crab Spectrum

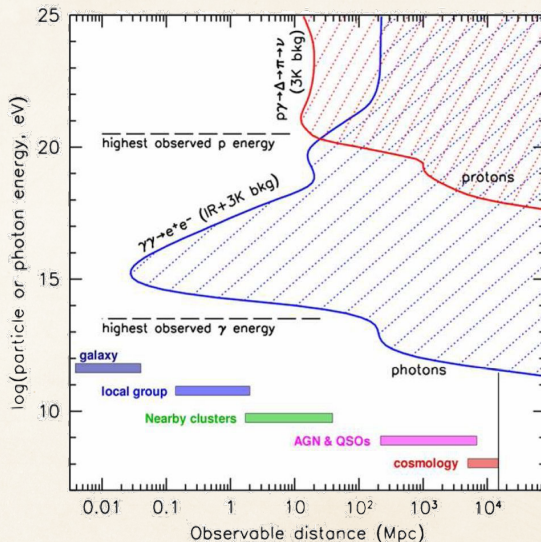


arXiv:1004.3098



Backup slides

Propagation of Gamma-Rays



arXiv:0902.3288



Backup slides

Galactic high energy sources

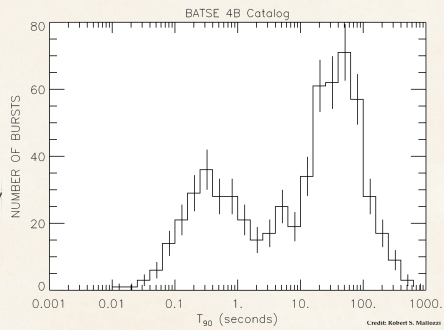
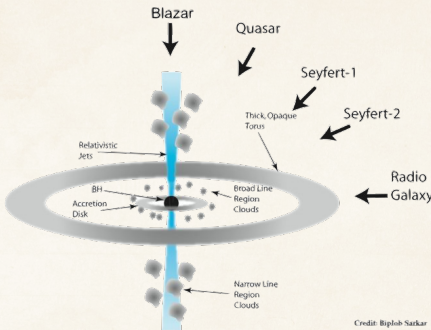


Main galactic source : SNR, PWN, binary systems



Backup slides

Extra-galactic high energy sources

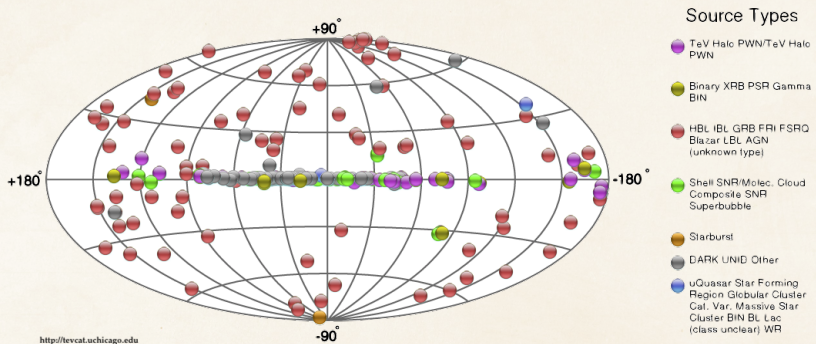


Main extra-galactic source : AGN, GRB



Backup slides

High energy sources map

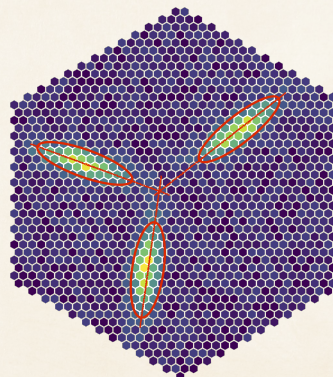
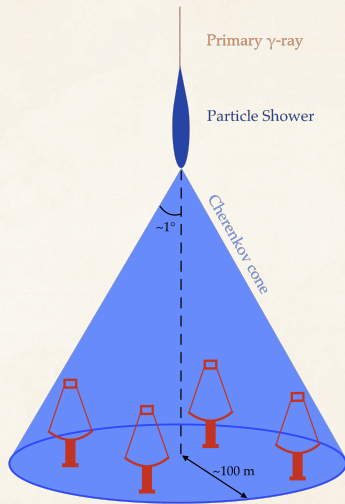


<http://tevcat.uchicago.edu>



Backup slides

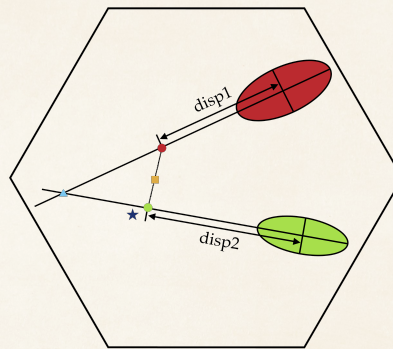
IACT: Stereoscopic measurements





Backup slides

IACT: Source position with a single telescope



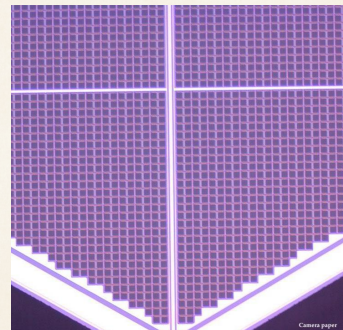
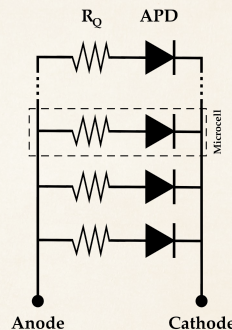
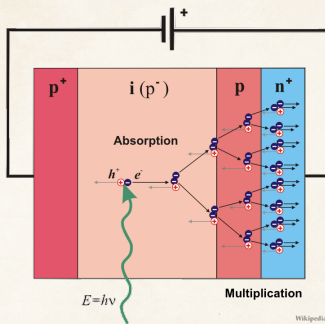
Reconstruction of the source position along the shower axis:

$$\text{disp} = \text{sign}(\text{skewness}) \cdot \xi \cdot \left(1 - \frac{\text{width}}{\text{length}}\right)$$



Backup slides

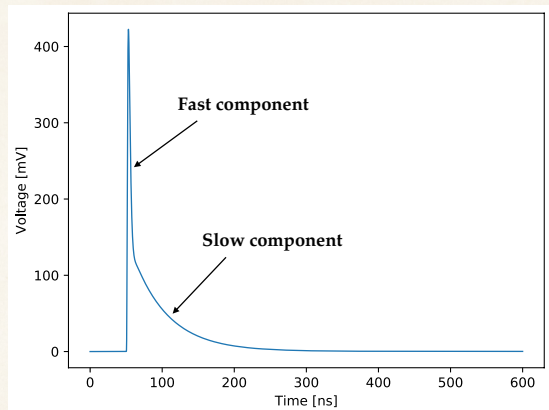
Silicon PhotoMultipliers (SiPM)





Backup slides

SiPM pulse shape model (Corsi)

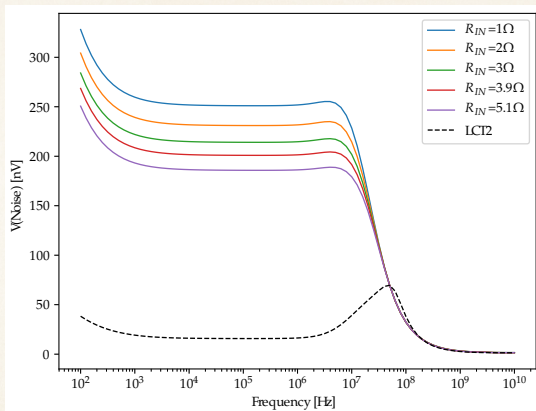


- Rising part : $\tau_{\text{rise}} = R_s \cdot C_d$
- Falling part : $\tau_{\text{fall,fast}} = R_s \cdot (C_q + C_g)$, $\tau_{\text{fall,slow}} = R_q \cdot (C_q + C_d)$
- Recovery time : $\tau_{\text{RC}} = C_d(R_q + R_s \cdot N)$



Backup slides

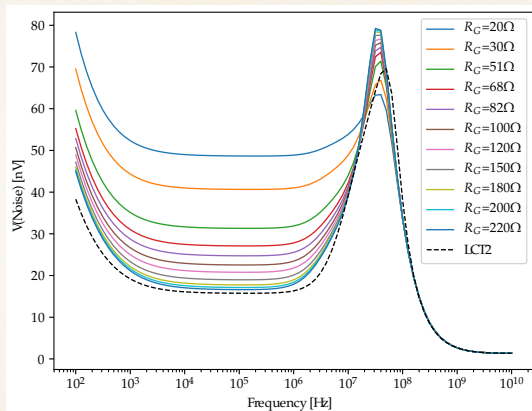
Evolution of noise with R_{IN}





Backup slides

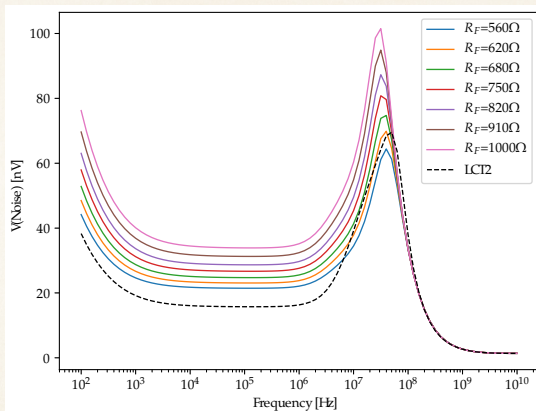
Evolution of noise with R_G





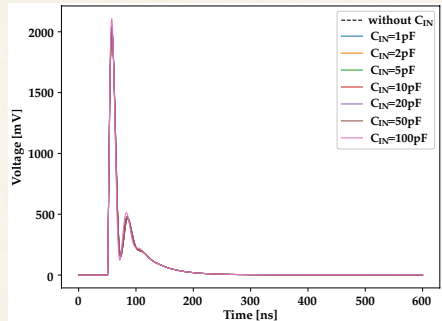
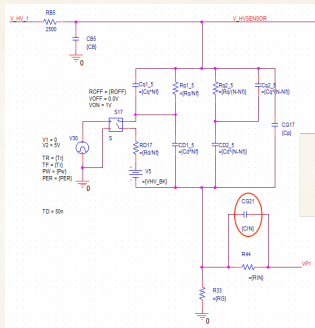
Backup slides

Evolution of noise with R_F



Backup slides

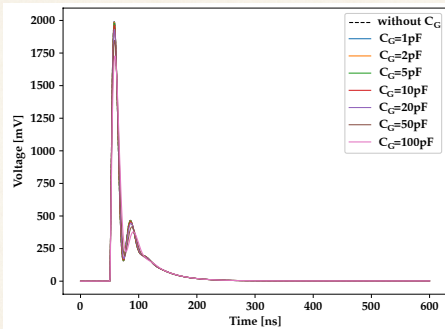
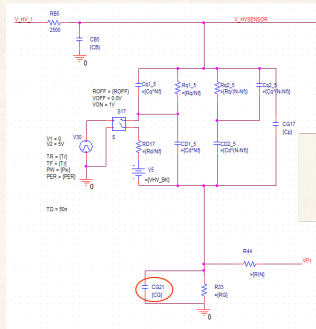
Evolution of the pulse shape with C_{IN}





Backup slides

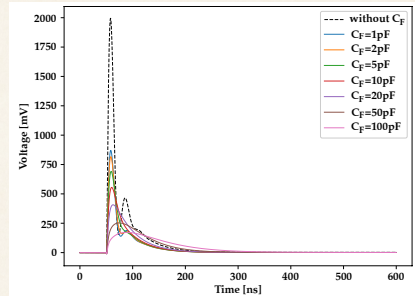
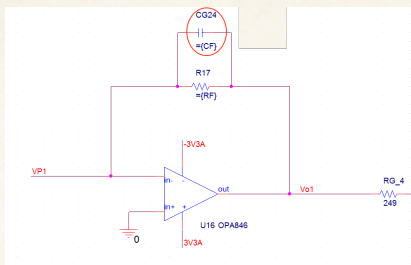
Evolution of the pulse shape with C_G





Backup slides

Evolution of the pulse shape with C_F

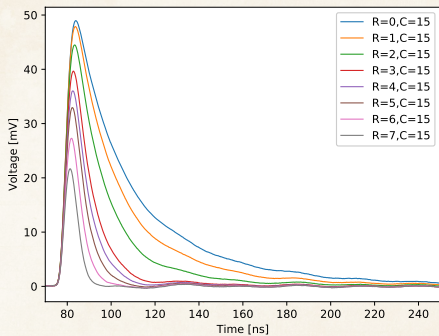




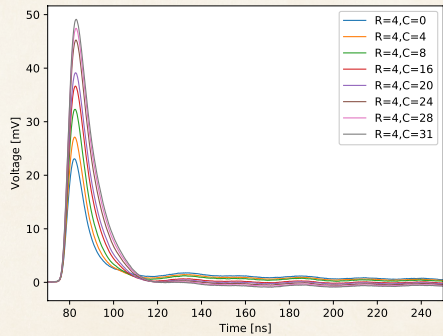
Backup slides

Pulse shape evolution with PZ parameters

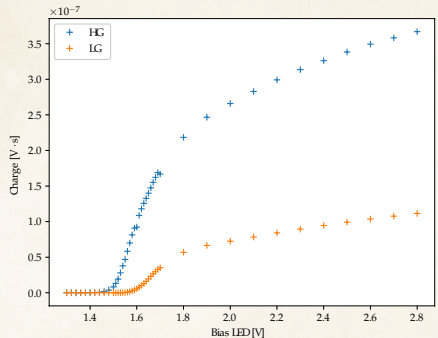
Varying R



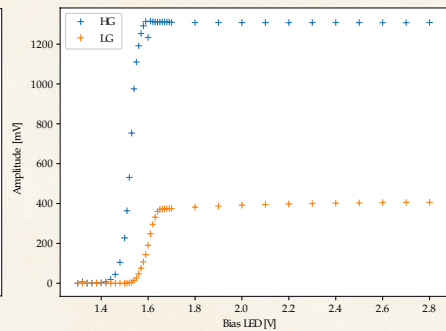
Varying C



Charge



Amplitude

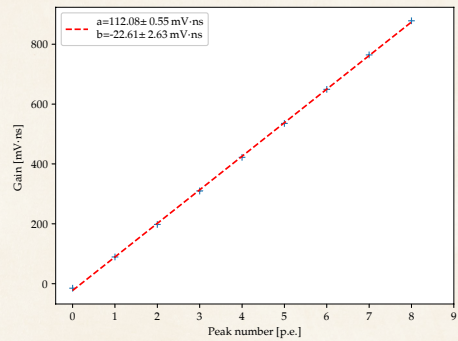
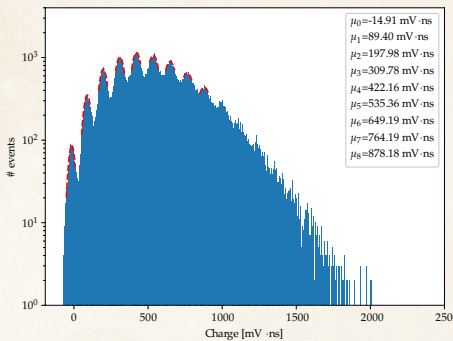


- Charge and amplitude as a function of LED bias voltage → LED calibration has to be performed in order to plot the behavior with the real light level



Backup slides

LED calibration

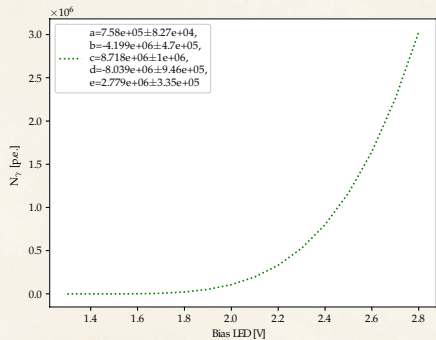
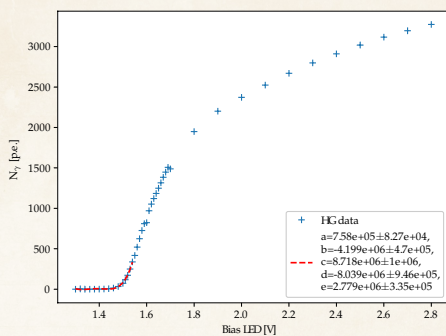


- Charge: $\text{gain}(\text{charge}) = 112 \text{ mV}\cdot\text{ns}$
- Amplitude: $\frac{\text{mean}(\text{charge})}{\text{gain}(\text{charge})} = 5.05 \text{ p.e.} \implies \frac{\text{mean}(\text{amplitude})}{5.05 \text{ p.e.}} = 3.4771 \text{ mV}$



Backup slides

LED calibration (for the charge)

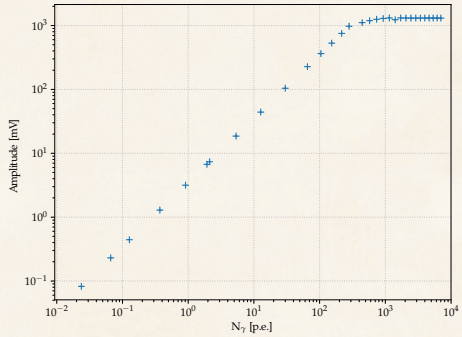
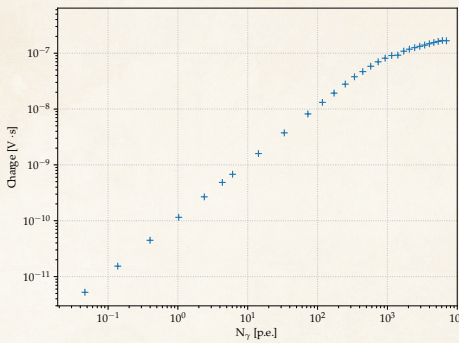


- 4-polynom fit of the non-saturated part in order to describe the LED behavior with increasing bias voltage



Backup slides

Linearity LCT5: Light level scan

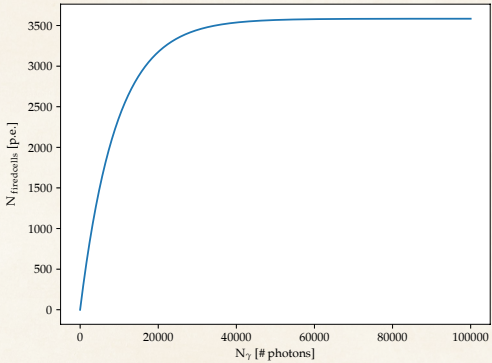
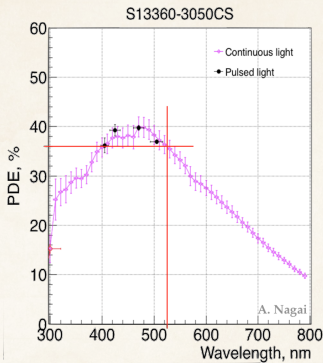


- Linearity behavior seems good
- Now the geometrical saturation of the sensor has to be accounted for



Backup slides

Linearity LCT5: Geometrical saturation



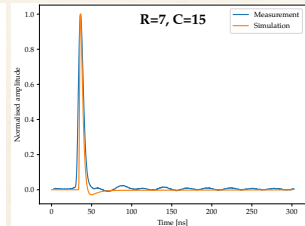
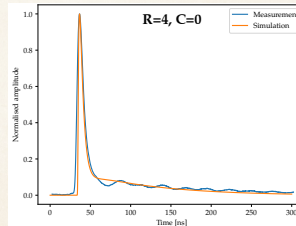
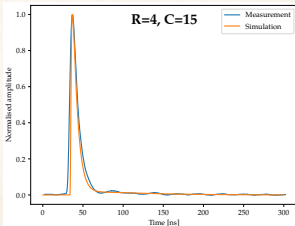
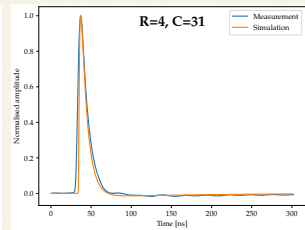
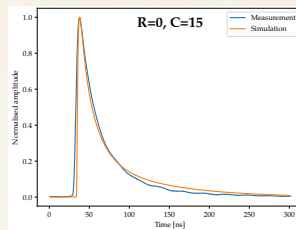
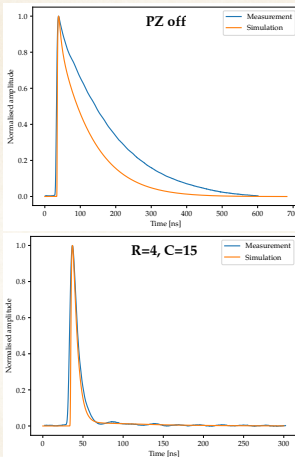
$$N_{\text{fired}} = N_{\text{total}} \left(1 - e^{-\frac{N_{\text{photons}} PDE(1+P_{XT})}{N_{\text{total}}}} \right)$$

- P_{XT}=8%
- N_{total}=3584 cells
- λ_{LED}=525 nm \implies PDE=36%



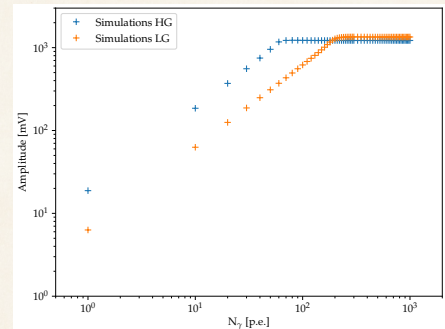
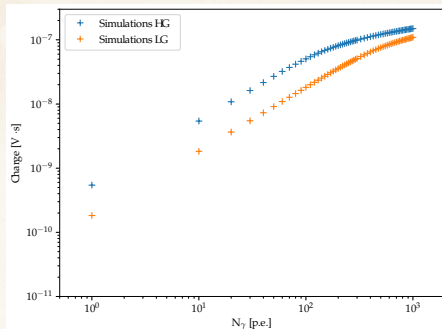
Backup slides

Simulation of MUSIC LVR3 pulse shapes



Backup slides

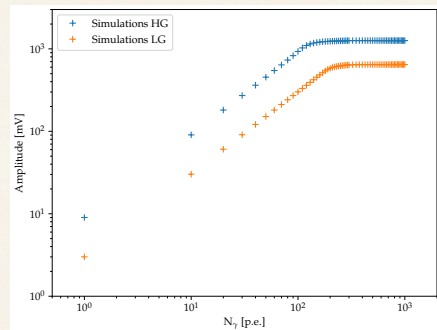
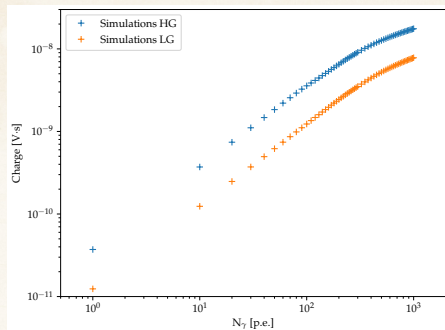
Simulation of MUSIC saturation (no PZC)





Backup slides

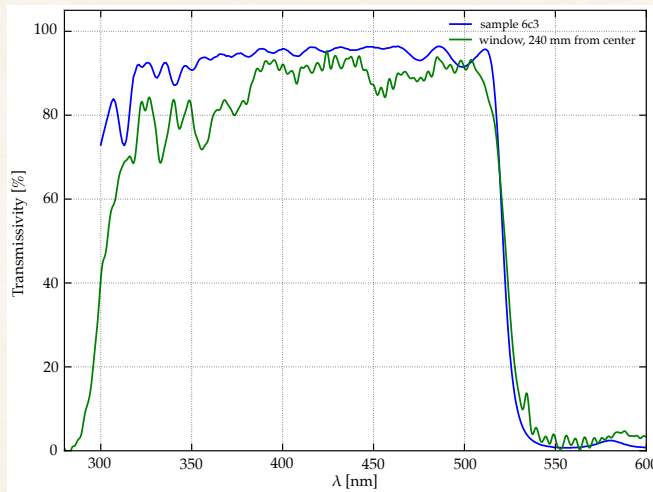
Simulation of MUSIC saturation (PZ: R=4, C=9)





Backup slides

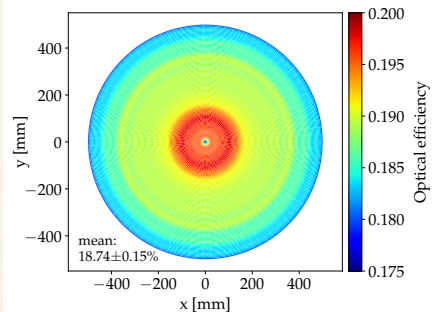
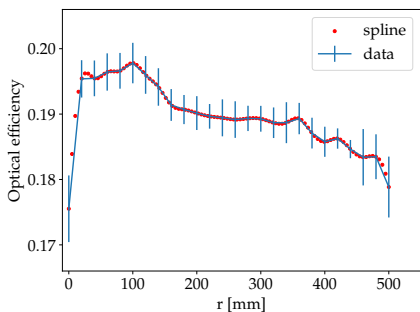
Comparison of the window spectrum with the sample





Backup slides

Extraction of the optical efficiency curve





Backup slides

Impact of non-uniformity on real data

Parameter	intensity	length	width	kurtosis
Mean relative difference	$-7.628 \cdot 10^{-4}$	$-1.379 \cdot 10^{-4}$	$-6.099 \cdot 10^{-4}$	$5.494 \cdot 10^{-4}$
Standard deviation	$3.766 \cdot 10^{-2}$	$4.962 \cdot 10^{-2}$	$2.470 \cdot 10^{-2}$	$2.287 \cdot 10^{-2}$
Parameter	r [mm]	ϕ [rad]	ψ [rad]	
Mean absolute difference	$-1.325 \cdot 10^{-1}$	$-1.797 \cdot 10^{-4}$	$-1.062 \cdot 10^{-3}$	
Standard deviation	2.049	$7.422 \cdot 10^{-2}$	$2.518 \cdot 10^{-1}$	
Parameter	skewness [mm]	alpha [rad]	miss [mm]	
Mean absolute difference	$8.464 \cdot 10^{-4}$	$-3.974 \cdot 10^{-4}$	$-2.419 \cdot 10^{-1}$	
Standard deviation	$5.939 \cdot 10^{-2}$	$4.438 \cdot 10^{-2}$	$1.032 \cdot 10^1$	



Backup slides

Impact of non-uniformity on simulated showers

Parameter	intensity	length	width	kurtosis
Mean relative difference	$8.265 \cdot 10^{-2}$	$3.600 \cdot 10^{-1}$	$1.018 \cdot 10^{-1}$	$3.089 \cdot 10^{-2}$
Standard deviation	$2.737 \cdot 10^{-1}$	1.152	$3.730 \cdot 10^{-1}$	$2.688 \cdot 10^{-1}$

Parameter	r [mm]	ϕ [rad]	ψ [rad]
Mean absolute difference	-1.522	$-5.978 \cdot 10^{-4}$	$1.634 \cdot 10^{-3}$
Standard deviation	$2.592 \cdot 10^1$	$7.279 \cdot 10^{-1}$	$5.525 \cdot 10^{-1}$

Parameter	skewness [mm]	alpha [rad]	miss [mm]
Mean absolute difference	$-2.564 \cdot 10^{-3}$	$6.202 \cdot 10^{-2}$	5.340
Standard deviation	$4.900 \cdot 10^{-1}$	$2.801 \cdot 10^{-1}$	$3.257 \cdot 10^1$